Ab Initio Calculations on the 5-*exo* versus 6-*endo* Cyclization of 1,3-Hexadiene-5-yn-1-yl Radical: Formation of the First Aromatic Ring in Hydrocarbon Combustion

Santiago Olivella*,†,‡ and Albert Solé†

Contribution from the Centre de Recerca en Química Teòrica, Departaments de Química Física i Química Orgànica, Universitat de Barcelona, Martí i Franqùes 1, 08028-Barcelona, Catalonia, Spain, and Institut d'Investigacions Químiques i Ambientals de Barcelona, Consell Superior d'Investigacions Científiques, Jordi Girona 18, 08034-Barcelona, Catalonia, Spain

Received March 21, 2000. Revised Manuscript Received September 13, 2000

Abstract: Two possible reaction pathways between 1,3-hexadien-5-yn-1-yl radical (**1**) and phenyl radical (**2**), a key reaction in soot formation during fuel combustion processes, have been investigated using ab initio quantum mechanical electronic structure calculations. The complete active space (CAS) SCF method was used for geometry optimization of the equilibrium and transition-state structures relevant to the two competing mechanisms and computing their harmonic vibrational frequencies. Final energies were evaluated by single-point calculations using essentially the G2M(RCC,MP2) method and corrected for zero-point and temperature effects. According to all calculated barrier heights ($\Delta U^{\ddagger}$, $\Delta E^{\ddagger}$, $\Delta H^{\ddagger}$, and $\Delta G^{\ddagger}$) the 5-*exo* cyclization of **1** to (2,4-cyclopentadienyl)vinyl radical (**3**) is favored over the 6-*endo* cyclization to **2**. As in the case of the prototypical hex-5-enyl radical, the predicted highly regioselective 5-*exo* cyclization of **1** is due to favorable enthalpic and entropic factors associated with the formation of the smaller ring. Contrary to common belief, the lowest-energy pathway of the reaction **1** → **2** is the 5-*exo* cyclization of **1** to **3** followed by cyclization of **3** to bicyclo[3.1.0]hex-3,5-dien-2-yl radical (**4**) and subsequent opening of the three-membered ring of **4** to yield **2**. The simple (one-step) 6-*endo* cyclization of **1** affording **2** requires a higher free energy of activation ($\Delta\Delta G^{\ddagger} = 1.5$ kcal/mol at 298 K) than such a stepwise cyclization. In light of these results, the stepwise reaction pathway found between **1** and **2** should be included in the set of reactions used in detailed kinetic modeling of soot formation in shock-tube studies of acetylene pyrolysis.

Introduction

The formation of the first aromatic ring (i.e., benzene and phenyl radical) is commonly believed to be the main reaction bottleneck in the formation of polycyclic aromatic hydrocarbons (PAHs) in hydrocarbon combustion.[1] PAHs are thought to be the precursors to soot particles[2,3] and constitute an important class of undesirable pollutants, many of which have been found to be mutagenic and carcinogenic.[4−7]

Thermal closure of 1,3-hexadien-5-yn-1-yl radical (**1**) is widely believed to constitute the major pathway in the formation of phenyl radical (**2**) along the stepwise addition of acetylenes

1 **2**

that presumably occurs in flames of small unsaturated hydrocarbons.[8] While several theoretical calculations have been reported on the concerted trimerization of acetylene to form benzene,[9−15] only a few theoretical papers have been devoted to the study of stepwise acetylene additions involving free radical species.[16,17] Specifically, the ring closure of **1** to give **2**

* Address correspondence to this author at the Departament de Química Orgànica. Fax: +34-93-3397878. E-mail: olivella@qo.ub.es.
† Universitat de Barcelona.
‡ Consell Superior d'Investigacions Científiques.

(1) (a) Frenklach, M.; Clary, D. W.; Gardiner, W. C., Jr.; Stein, S. E. *20th Symposium (International) on Combustion;* The Combustion Institute: Pittsburgh, PA, 1984; p 887−901. (b) Frenklach, M. *22nd Symposium (International) on Combustion;* The Combustion Institute: Pittsburgh, PA, 1988; p 1159. (c) Frenklach, M.; Warnatz, J. *Combust. Sci. Technol.* **1987**, *51,* 265.
(2) Haynes, B. S.; Wagner, H. G. *Prog. Energy Combust. Sci.* **1981**, *7,* 229.
(3) Calcote, H. F. *Combust. Flame* **1981**, *42,* 215.
(4) (a) Longwell, J. P. *20th Symposium (International) on Combustion;* The Combustion Institute: Pittsburgh, PA, 1982; p 1339. (b) Longwell, J. P. In *Soot in Combustion System and its Toxic Properties;* Lahaye, J., Prado, G., Eds.; Plenum: New York, 1983; p 37.
(5) Thilly, W. G. In *Soot in Combustion System and its Toxic Properties;* Lahaye, J., Prado, G., Eds.; Plenum: New York, 1983; p 1.
(6) Lowe, J. P.; Silverman, B. D. *Acc. Chem. Res.* **1984**, *17,* 332.
(7) Ball, L. M.; Warren, S. H.; Sangaiah, R.; Nesnow, S.; Gold, A. *Mutation Res.* **1989**, *224,* 115.
(8) Miller, J. A.; Mellius, C. F. *Combust. Flame* **1992**, 21.
(9) Houk, K. N.; Gandor, R. W.; Rondan, N. G.; Paquette, L. A. *J. Am. Chem. Soc.* **1979**, *101,* 6797.
(10) Bach, R. D.; Wolber, J. W.; Schlegel, H. B. *J. Am. Chem. Soc.* **1985**, *107,* 2837.
(11) Ioffe, A.; Shaik, S. *J. Chem. Soc., Perkin Trans. 2* **1992**, 2101.
(12) Wagenseller, P. E.; Birney, D. M.; Roy, D. *J. Org. Chem.* **1995**, *60,* 2853.
(13) Jiao, H. J.; Schleyer, P. v. R. *J. Phys. Org. Chem.* **1998**, *11,* 655.
(14) Morao, I.; Cossio, F. P. *J. Org. Chem.* **1999**, *64,* 1868.
(15) Cioslowski, J.; Liu, G.; Moncrieff, D. *Chem. Phys. Lett.* **2000**, *316,* 536.

10.1021/ja001011v CCC: $19.00
Published on Web 11/03/2000

Scheme 1

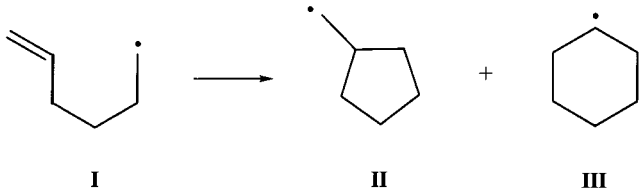

I **II** **III**

98% 2%

has been studied theoretically by Walch[17] as one of the possible elementary reactions involved in the ring-closure reactions of $C_4H_3^{\bullet}$ radical species with acetylene. Employing single-point internally contracted configuration interaction (ICCI) calculations with the Dunning correlation consistent polarized valence double-ζ basis set (cc-pVDZ), performed at the geometries optimized by using the restricted open-shell Hartree−Fock (ROHF) method with a double-ζ basis set, Walch find an energy barrier of 7.1 kcal/mol (including the zero-point effects) for the ring closure of **1** leading to **2**. This value is substantially lower than the semiempirical MINDO/3 value of 16.6 kcal/mol computed by Dewar et al.[18] Recently, Lin and co-workers[19] reported a theoretical investigation on the unimolecular decomposition of **2**, employing a modified Gaussian-2 method.[20] The energy barrier for decyclization of **2** to **1** was calculated to be 66.5 kcal/mol with the corresponding recyclization barrier energy of 5.6 kcal/mol, which compares reasonably well with the value of 7.1 kcal/mol obtained by Walch.

At this point it is worth comparing the cyclization of **1** with the analogous ring closure of the prototypical hex-5-en-1-yl radical (**I**). The latter process occurs regiospecifically in the 5-*exo* mode affording mainly cyclopentylmethyl radical (**II**), as shown in Scheme 1. The overwhelming preference for 5-*exo* ring closure **I** → **II** over the 6-*endo* cyclization, which gives cyclohexyl radical (**III**), is a consequence of the interplay of three main factors, the stereoelectronic, polar, and steric effects.[21] All three effects favor production of **II**, the less thermodynamically stable of the two possible products. On the basis of these results one would expect the ring closure of **1** to occur also regiospecifically in the 5-*exo* fashion affording mainly (2,4-cyclopentadienyl)vinyl radical (**3**) rather than the 6-*endo* cyclized product **2**. Interestingly, in his theoretical study of the

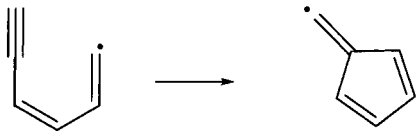

1 **3**

ring-closure reactions of $C_4H_3^{\bullet}$ radicals with acetylene, Walch finds an energy barrier of 36.7 kcal/mol for the ring opening of **3** to give **1**. From the relative energies reported by Walch, an energy barrier of 3.4 kcal/mol is obtained for the reverse 5-*exo* ring closure **1** → **3**. Therefore, the energy barrier for the 5-*exo* cyclization **1** → **3** is predicted to be less than a half of the barrier (7.1 kcal/mol) for the 6-*endo* ring closure **1** → **2**. Accordingly, it seems unlikely that **2** is formed by simple 6-*endo* cyclization of **1** in the combustion of small unsaturated hydrocarbons.

Since there possibly are alternative mechanisms not considered previously, here we present the results of our theoretical investigation of a part of the ground-state $C_6H_5^{\bullet}$ potential energy surface (PES), in an attempt to clarify how **2** is formed from **1**.

Methods and Computational Details

The geometries of the relevant stationary points on the ground-state $C_6H_5^{\bullet}$ PES were initially optimized by using the spin-unrestricted Hartree−Fock (UHF) version of the self-consistent field (SCF) molecular orbital (MO) method[22] with the d-polarized split-valence 6-31G(d) basis set[23] employing analytical gradient procedures.[24,25] All of these ab initio calculations were performed with the GAUSSIAN 94 program package.[26]

The UHF wave function of the calculated structures was subjected to very serious spin contamination, S^2 ranging from 1.4715 to 2.1127 as compared to 0.75 for a pure doublet state. This can be taken as an indication of strong nondynamical electron correlation effects. One may then question the reliability of the geometries calculated at the UHF level of theory for these structures. Accordingly, all of the geometries (minima and saddle points) were reoptimized by use of multiconfiguration SCF (MCSCF) wave functions of the complete active space (CAS) SCF class[27] with the 6-31G(d) basis set employing analytical gradient procedures.[25,28] The CASs were selected following the procedure suggested by Pulay and Hamilton,[29] based on the fractional occupation of the natural orbitals of the UHF wave function (designated UNOs). These indicated a number of *active* orbitals which varied from 5, for the structure **4**, to 9, for the structures **1**, **TS-1/2**, and **TS-1/3**. The distribution among the *active* orbitals of the same number of *active* electrons led in each case to CASSCF wave functions formed as a linear combination of a number of doublet spin-adapted configuration state functions which varied from 75 (**4**) to 8820 (**1**, **TS-1/2**, and **TS-1/3**). All CASSCF geometry optimizations were carried out by using GAMESS system of programs.[30]

All of the stationary points were characterized by their harmonic vibrational frequencies as minima or saddle points. The harmonic vibrational frequencies were obtained by diagonalizing the mass-weighted Cartesian force constant matrix calculated analytically at the CASSCF level of theory with the 6-31G(d) basis set by using GAUSSIAN 94. Connections of the transition structures between designated minima were confirmed by intrinsic reaction coordinate (IRC) calculations[31] at the CASSCF/6-31G(d) level using the second-order algorithm of Gonzalez and Schlegel[32] implemented into GAMESS, with a step size of 0.15 bohr·amu$^{1/2}$.

(16) (a) Gey, E.; Wiegratz, S.; Ondruschka, B. *Z. Prakt. Chem.* **1989**, *270*, 1067. (b) Ha, T.-K.; Gey, E. *J. Mol. Struct. (THEOCHEM)* **1994**, *306*, 197.

(17) Walch, S. P. *J. Chem. Phys.* **1995**, *103*, 8544.

(18) Dewar, M. J. S.; Gardiner, W. C., Jr.; Frenklach, M., Oref, I. *J. Am. Chem. Soc.* **1987**, *109*, 4456.

(19) Madden, L. K.; Moskaleva, L. V.; Lin, M. C. *J. Phys. Chem A* **1997**, *101*, 6790.

(20) Mebel, A. M., Morokuma, K.; Lin, M. C. *J. Chem. Phys.* **1995**, *103*, 7414.

(21) For leading references, see: (a) Beckwith, A. L. J. *Chem. Soc. Rev.* **1993**, *22*, 143. (b) RajanBabu, T. V. *Acc. Chem. Res.* **1991**, *24*, 139. (c) Beckwith, A. L. J. *Tetrahedron* **1981**, *37*, 3073. (d) Giese, B. *Ang, Chem., Int. Ed. Engl.* **1983**, *22*, 753. (e) Julia, M *Acc. Chem. Res.* **1971**, *4*, 386. (f) Giese, B. In *Radicals in Organic Synthesis: Formation of Carbon-Carbon Bonds*; Baldwin, J. E., Ed., Pergamon: New York, 1986.

(22) Pople, J. A.; Nesbet, R. K. *J. Chem. Phys*. **1954**, *22*, 571.

(23) (a) Hehre, W. J.; Ditchfield, R.; Pople, J. A. *J. Chem. Phys.* **1972** *56*, 2257. (b) Hariharan, P. C.; Pople, J. A. *Theor. Chim. Acta*. **1973**, *28*, 213.

(24) Schlegel, H. B. *J. Comput. Chem*. **1982**, *3*, 214.

(25) Bofill, J. M. *J. Comput. Chem.* **1994**, *15*, 1.

(26) Frisch, M. J.; Trucks, G. W.; Schlegel, H. B.; Gill, P. M. W.; Johnson, B. G.; Robb, M. A.; Cheeseman, J. R.; Keith, T. A.; Petersson, G. A.; Montgomery, J. A.; Raghavachari, K.; Al-Laham, M. A.; Zakrzewski, V. G.; Ortiz, J. V.; Foresman, J. B.; Cioslowski, J.; Stefanov, A.; Nanayakkara, A.; Challacombe, M.; Peng, C. Y.; Ayala, P. Y.; Chen, W.; Wong, M. W.; Andres, J. L.; Replogle, E. S.; Gomperts, R.; Martin, R. L.; Fox, D. J.; Binkley, J. S.; Defrees, D. J.; Baker, J.; Stewart, J. J. P.; Head-Gordon, M.; Gonzalez, C.; Pople, J. A. *GAUSSIAN 94*; Gaussian, Inc.: Pittsburgh, PA, 1995.

(27) For a review, see: Roos, B. O. *Adv. Chem. Phys*. **1987**, *69*, 399.

(28) (a) Baker, J. *J. Comput. Chem.* **1986**, *7*, 385. (b) Baker, J. *J. Comput. Chem.* **1987**, *8*, 563.

(29) Pulay, P.; Hamilton, T. P. *J. Chem. Phys*. **1988**, *88*, 4926.

(30) Schmidt, M. W.; Baldrige, K. K.; Boatz, J. A.; Elbert, S. T.; Gordon, M. S.; Jensen; J.; Koseki, S.; Matsunaga, N.; Nguyen, K. A.; Su, S.; Windus, T. L.; Dupuis, M.; Montgomery, J. A. *J. Comput. Chem.* **1993**, *14*, 1347.

With the aim of assessing the performance of current density functional theory (DFT) for the description of intramolecular free radical cyclization reactions, geometries and harmonic vibrational frequencies of the stationary points located on the CASSCF PES were also calculated using the Becke three-parameter hybrid functional[33] combined with the Lee, Yang, and Parr (LYP) correlation functional, [34] designed B3LYP,[35] employing the 6-31G(d) basis set. To establish that our results were converged with respect to basis set, single-point B3LYP calculations were carried out with the split-valence 6-311+G(3df,2p) basis set,[36] which includes a single diffuse sp shell on heavy atoms, triple d-polarization and a single additional f-polarization on heavy atoms, and double p-polarization on hydrogen atoms. The B3LYP calculations were carried out with the GAUSSIAN 94 program.

To incorporate the effect of dynamical valence-electron correlation on the relative energy ordering of the stationary points located at the CASSCF/6-31G(d) level, overall energetics were determined by single-point (frozen-core) calculations using essentially the modified Gaussian-2 method,[37] G2M(RCC,MP2), of Mebel et al.[20] The three deviations between our calculations and the G2M(RCC,MP2) method as described in ref 12 are (1) our use of geometries determined at the CASSCF/6-31G(d) level instead of the B3LYP/6-311G(d,p) level, (2) our use of zero-point vibrational energy (ZPVE) corrections based on CASSCF/6-31G(d) frequencies instead of B3LYP/6-311G(d,p) frequencies, and (3) our non-use of higher-level correction. The G2M(RCC,MP2) scheme includes a series of calculations to approximate a restricted open shell coupled-cluster[38] calculation including all single and double excitations, based on a restricted open-shell Hartree−Fock reference determinant, together with a perturbative treatment of all connected triple excitations,[39] denoted RCCSD(T), with the 6-311+G(3df,2p) basis set. In the present work the RCCSD(T)/6-311+G(3df,2p) energy was approximated by using the expression

$$E[\text{RCCSD(T)/6-311+G(3df,2p)}] \approx E[\text{RCCSD(T)/6-311G(d,p)}] + E[\text{PUMP2/6-311+G(3df,2p)}] - E[\text{PUMP2/6-311G(d,p)}] \quad (1)$$

where PUMP2 stands for spin-projected[40] second-order unrestricted Møller−Plesset perturbation theory.[41] This additivity approximation has been tested previously[20] and found to provide a useful approach when direct RCCSD(T)/6-311+G(3df,2p) calculations are not feasible. The PUMP2 calculations were carried out with the GAUSSIAN 94 program, whereas MOLPRO 98[42] program package was employed for the RCCSD(T) calculations.

Relative energies discussed in the text refers to approximated RCCSD(T)/6-311+G(3df,2p) unless stated otherwise. ZPVEs were determined from unscaled harmonic vibrational frequencies calculated at both the CASSCF/6-31G(d) and B3LYP/6-31G(d) levels of theory.

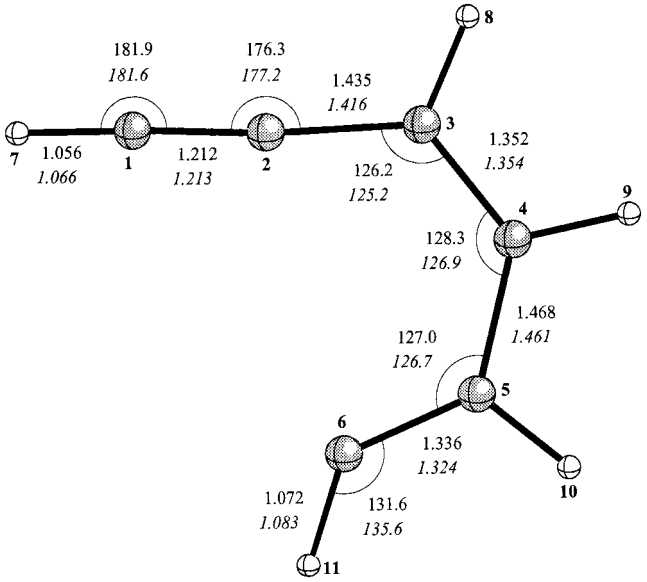

1, C_s

Figure 1. Selected parameters of the CASSCF/6-31G(d)-optimized geometry of 1,3-hexadien-5-yn-1-yl radical (**1**). The B3LYP/6-31G(d)-optimized geometrical parameters are given in italics. Distances are given in Å and angles in deg.

Our best total energies at 0 K correspond to the sum of the approximated RCCSD(T)/6-311+G(3df,2p) energy and ZPVE correction. Thermal corrections to enthalpy and Gibbs free energy values, as well as the absolute entropies, were obtained, assuming ideal gas behavior, from unscaled harmonic frequencies and moments of inertia by standard methods.[43] A standard pressure of 1 atm was taken in the entropy calculations.

For both 5-*exo* and 6-*endo* cyclization of **1** the dependence of the unimolecular rate constant $k(E)$ on the internal energy E of a reactant molecule was calculated on the basis of standard RRKM theory of unimolecular reactions, which can be formulated as[44]

$$k(E) = \frac{W^t(E - E_0)}{\hbar\rho(E)} \quad (2)$$

where E_0 is the critical energy of the reaction (i.e., the energy barrier including the ZPVE), $W^t(E - E_0)$ is the total number of states of the transition state within the energy interval $E - E_0$, $\rho(E)$ is the density of states of the reactant molecule, and $\hbar$ is Planck's constant. $W^t(E - E_0)$ and $\rho(E)$ were enumerated by direct count of vibrational states using a program[45] based on the Beyer−Swinehart algorithm.[44,46]

The RRKM computations employed the potential energy barriers calculated at the approximated RCCSD(T)/6-311+G(3df,2p) level and the unscaled CASSCF/6-31G(d) harmonic vibrational frequencies. The torsional modes were treated as low-frequency vibrations.

Results and Discussion

Selected geometrical parameters of the structures of reactant, products, intermediates, and transition states calculated in the present paper are shown in Figures 1−4 (bond lengths in Å, bond angles and dihedral angles in deg), which are computer-generated plots of the CASSCF/6-31G(d)-optimized geometries.[47] The optimized geometry of **2** is essentially the same as

(31) (a) Fukui, K. *Acc. Chem. Res.* **1981**, *14*, 363. (b) Ishida, K.; Morokuma, K.; Kormornicki, A. *J. Chem. Phys.* **1977**, *66*, 2153. (c) Schmidt, M. W.; Gordon, M. S.; Dupuis, M. *J. Am. Chem. Soc.* **1985**, *107*, 7, 2585.
(32) (a) Gonzalez, C.; Schlegel, B. *J. Chem. Phys.* **1989**, *90*, 2154. (b) Gonzalez, C.; Schlegel, B. *J. Phys. Chem.* **1990**, *94*, 5523.
(33) (a) Becke, A. D. *Phys. Rev. A* **1988**, *37*, 3098. (b) Becke, A. D. *J. Chem. Phys*. **1993**, *98*, 5648.
(34) Lee, C.; Yang, W.; Parr, R. G. *Phys. Rev. B* **1988**, *37*, 785.
(35) Stevens, P. J.; Devlin, F. J.; Chablowski, C. F.; Frisch, M. J. *J. Phys. Chem.* **1994**, *98*, 11623.
(36) Frisch, M. J.; Pople, J. A.; Binkley. J. S. *J. Chem. Phys.* **1984**, *80*, 3265.
(37) (a) Curtiss, L. A., Raghavachari, K.; Trucks, G. W.; Pople, J. A. *J. Chem Phys.* **1991**, *94*, 7221. (b) Curtiss, L. A., Raghavachari, K.; Pople, J. A. *ibid.***1993**, *98*, 1293.
(38) Knowles, P. J.; Hampel, C.; Werner, H.-J. *J. Chem. Phys.* **1993**, *99*, 5219.
(39) Raghavachari, K.; Trucks, G. W.; Pople. J. A.; Head-Gordon, M. *Chem. Phys. Lett.* **1989**, *157*, 479.
(40) Chen, W., Schlegel, H. B. *J. Chem. Phys.* **1994**, *101*, 5957.
(41) (a) Møller, C.; Plesset, M. *Phys. Rev.* **1934**, *46*, 618. (b) Pople, J. A.; Binkley, J. S.; Seeger, R. *Int. J. Quantum Chem., Symp.* **1976**, *10*, 1. (c) Krishnan, R.; Pople, J. A. *Int. J. Quantum Chem.* **1978**, *14*, 91.
(42) Werner, H.-J.; Knowles, P. J.; Amos, R. D.; Berning, A.; Cooper, D. L.; Deegan, M. J. O.; Dobbyn. A. J.; Eckert, S. T.; Hampel, C.; Leininger, C.; Lindh, R.; Lloyd, A. W.; Meyer, W.; Mura, M. E.; Nicklass, A.; Palmeiri, P.; Peterson, K. A.; Pitzer, R.; Pulay, P.; Rauhaut, G.; Schü tz. M.; Stoll, H.; Stone, A. J.; Thorsteinsson, T. MOLPRO, version 98.1; University of Stuttgart: 1998 Germany.
(43) See, e.g.: McQuarrie, D. *Statistical Mechanics;* Harper and Row: New York, 1986.
(44) Gilbert, R. G.; Smith, S. C. *Theory of Unimolecular and Recombination Reactions*; Blackwell Scientific Publications: Oxford, 1990.
(45) Solé, A., unpublished work.
(46) Beyer, T.; Swinehart, D. F. *Commun. ACM* **1973**, *16*, 379.
(47) Full set of Cartesian coordinates for all structures as obtained by CASSCF and B3LYP methods is available upon request from the authors.

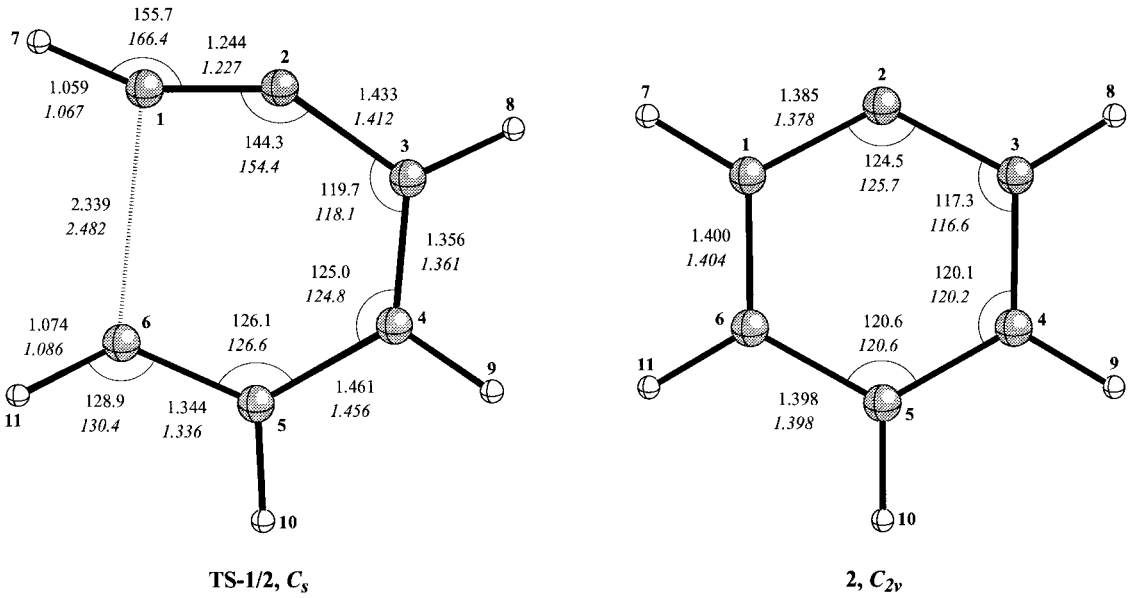

TS-1/2, C_s **2, C_{2v}**

Figure 2. Selected parameters of the CASSCF/6-31G(d)-optimized geometries of the transition structure (**TS-1**/**2**) for the 6-*endo* cyclization of **1** and the phenyl radical (**2**). The B3LYP/6-31G(d) optimized geometrical parameters are given in italics. Distances are given in Å and angles in deg.

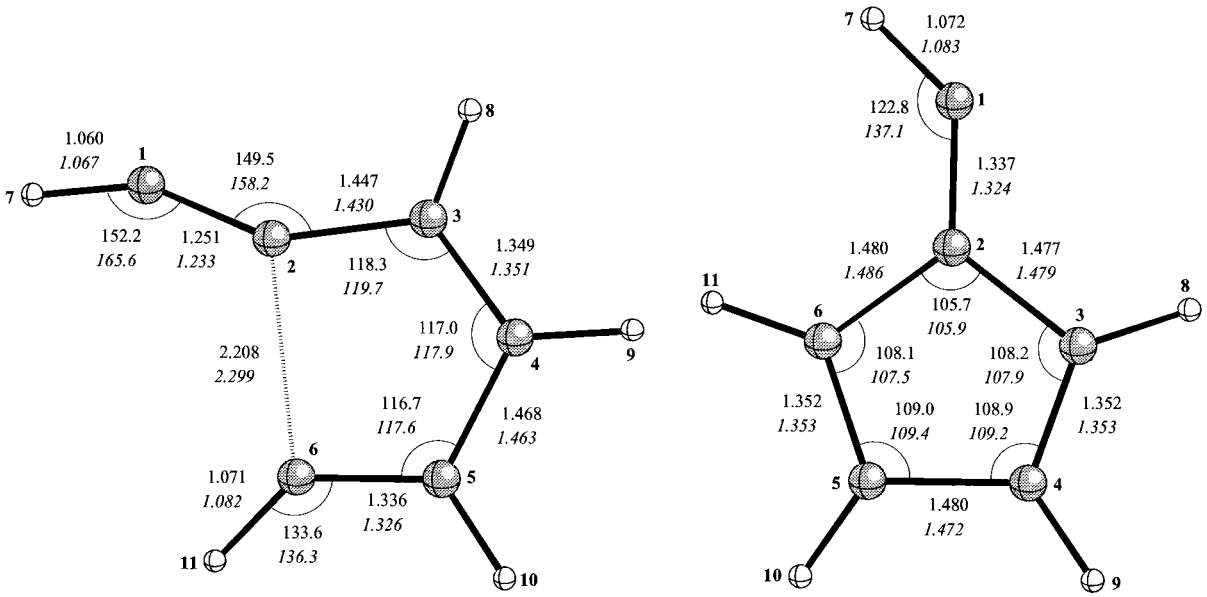

TS-1/3, C_s **3, C_s**

Figure 3. Selected parameters of the CASSCF/6-31G(d)-optimized geometries of the transition structure (**TS-1**/**3**) for the 5-*exo* cyclization of **1** and the (2,4-cyclopentadienyl)vinyl radical (**3**). The B3LYP/6-31G(d) optimized geometrical parameters are given in italics. Distances are given in Å and angles in deg.

that calculated by Squires and co-workers[48] at the CASSCF(7,7)/3-21G(d) level. For the purpose of comparison, the values of the geometrical parameters for the structures optimized at the B3LYP/6-31G(d) level of computation are also given in italics in Figures 1−4. Some B3LYP/6-31G(d)-optimized structures (i.e., **1**, **2**, and **TS-1/2**) have been reported previously.[19] Overall, the structures calculated at the CASSCF level of theory are similar to those optimized with the B3LYP method. Relative energies obtained at the approximated RCCSD(T)/6-311+G(3df,2p) level (ΔU) are given in Table 1. In addition, Table 1 includes the relative ZPVEs ($\Delta ZPVE$), as well as the relative energies at 0 K (ΔE) and the relative enthalpies (ΔH) and Gibbs free energies (ΔG) calculated at 298 and 1450 K. The latter temperature was chosen to represent a typical temperature used in shock-tube pyrolysis of acetylene.[1] The total energies calculated at various levels of theory with different basis sets are summarized in Table S1 (Supporting Information). Table S2 (Supporting Information) contains the ZPVEs, thermal corrections to enthalpy, and absolute entropies calculated for the CASSCF/6-31G(d)-optimized structures. The total energies, ZPVEs, thermal correction to enthalpy, and absolute entropies calculated for the B3LYP/6-31G(d)-optimized structures are given in Table S3 (Supporting Information). Finally, Figure 5 summarizes the energy profiles calculated at the approximated RCCSD(T)6-311+G(3df,2p) + ZPVE level for two different pathways leading to the formation of **2** from **1** found on the CASSCF PES.

(48) Wenthold, P. G.; Wierschke, S. G.; Nash, J. J.; Squires, R, R. *J. Am. Chem. Soc.* **1994**, *116*, 7378.

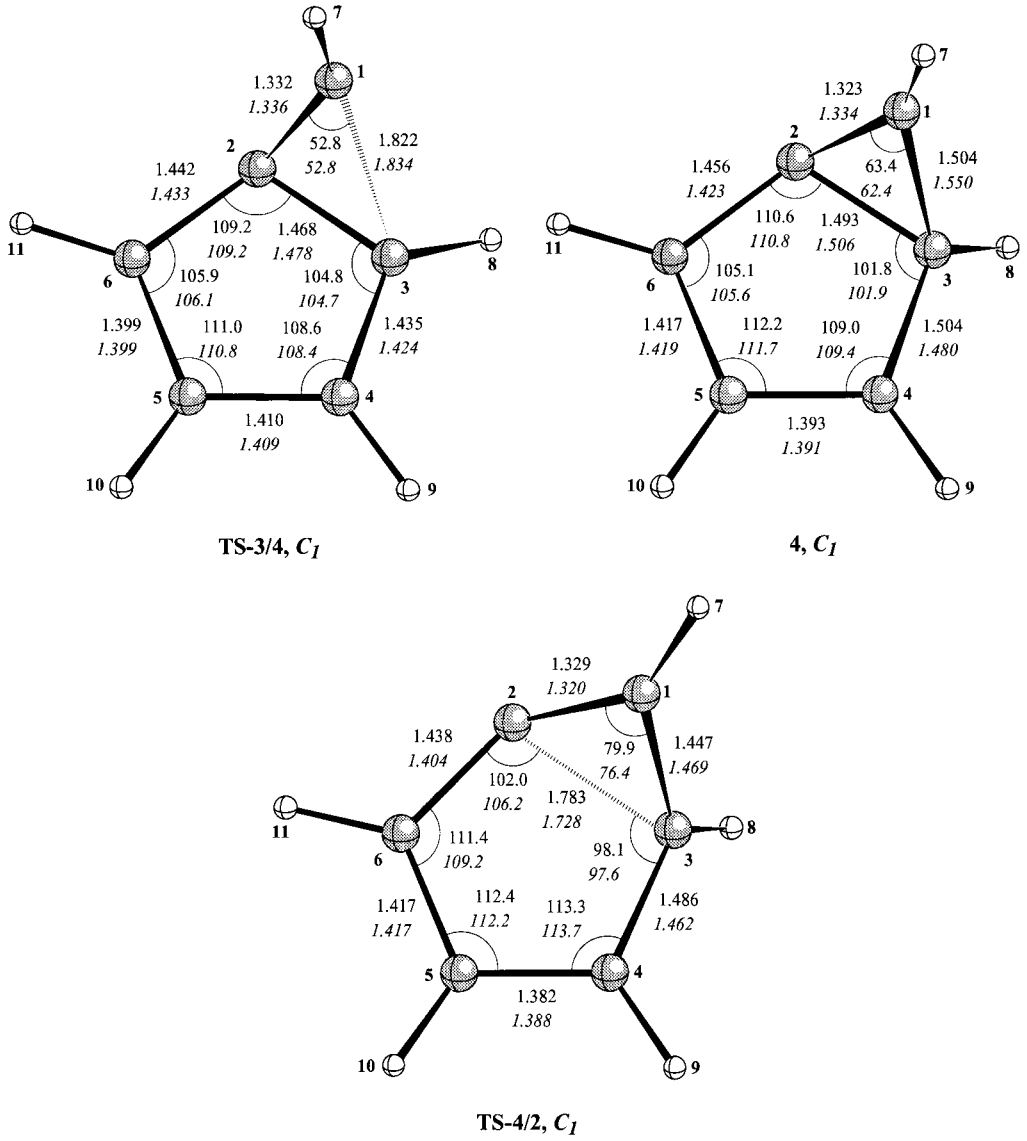

Figure 4. Selected parameters of the CASSCF/6-31G(d)-optimized geometries of the transition structure (**TS-3/4**) for the cyclization of **3**, the bicyclo[3.1.0]hex-3,5-dien-2-yl radical (**4**), and the transition structure for the three-membered ring opening of **4** to **2**. The B3LYP/6-31G(d)-optimized geometrical parameters are given in italics. Distances are given in Å and angles in deg.

Table 1. Calculated Relative Energies (kcal/mol) for CASSCF/6-31G(d)-Optimized Stationary Points on the $C_6H_5^\bullet$ Potential Energy Surface

stationary point	ΔU^a	ΔZPVE^b	ΔE (0 K)	ΔH (298 K)	ΔG (298 K)	ΔH (1450 K)	ΔG (1450 K)
1	0.0	0.0	0.0	0.0	0.0	0.0	0.0
TS-1/2	6.0	0.3	6.3	5.5	7.3	2.9	17.4
2	−66.6	5.2	−61.4	−62.9	−59.4	−65.9	−40.7
TS-1/3	5.1	−0.2	4.9	4.3	5.8	2.0	14.0
3	−35.2	3.0	−32.2	−33.3	−30.9	−35.0	−18.6
TS-3/4	−4.7	2.1	−2.6	−4.0	−1.0	−7.7	15.5
4	−7.2	2.8	−4.4	−5.6	−2.8	−7.3	11.3
TS−4/2	−1.3	1.3	0.0	−1.2	1.6	−4.5	16.8

[a] Relative energy at the approximated RCCSD(T)/6-311+G(3df,2p) level of theory, obtained using the G2M(RCC,MP2) computational scheme. [b] Differential zero-point vibrational energy corrections obtained from CASSCF/6-31G(d) calculated harmonic vibrational frequencies.

A. 5-*exo* *versus* 6-*endo* Cyclization of 1. The 6-*endo* ring closure of **1** to give **2** takes place via the transition structure labeled as **TS-1/2** in Figure 2. At 0 K this intramolecular radical addition is predicted to be exoergic by 61.4 kcal/mol. This value is in good agreement with the exoergicity of 60.9 kcal/mol obtained by Lin et al.[19] with the G2M(rcc,MP2) model but is 3.5 kcal/mol lower than the value of 64.9 kcal/mol obtained from the ICCI/cc-pVDZ + ZPVE relative energies reported by Walch.[17] The potential energy barrier ($\Delta U^\ddagger$) for 6-*endo* ring closure of **1** is calculated to be 6.0 kcal/mol. Inclusion of the ZPVE correction leads to a predicted activation energy at 0 K ($\Delta E^\ddagger$) of 6.3 kcal/mol. This $\Delta E^\ddagger$ compares reasonably well with the values of 7.1 and 5.6 kcal/mol obtained from the relative energies reported by Walch[17] and Lin et al.,[19] respectively.

The 5-*exo* ring closure of **1** to give **3** occurs through the transition structure labeled as **TS-1/3** in Figure 3. At 0 K the **1** → **3** cyclization is predicted to be exoergic by 32.2 kcal/mol. This value is in reasonable agreement with the exoergicity of 33.3 kcal/mol obtained from the relative energies reported by Walch.[17] The $\Delta U^\ddagger$ for the 5-*exo* ring closure of **1** is calculated to be 5.1 kcal/mol. Inclusion of the ZPVE correction leads to a predicted $\Delta E^\ddagger$ of 4.9 kcal/mol, which is somewhat higher than the value of 3.4 kcal/mol obtained from the relative energies reported by Walch.[17]

According to Table 1 **TS-1/3** is predicted to be less energetic than **TS-1/2**. Thus, the $\Delta U^\ddagger$ for the 5-*exo* cyclization **1** → **3** is 0.9 kcal/mol lower than for the 6-*endo* ring closure **1** → **2**. Inclusion of ZPVE corrections to energy and thermal corrections

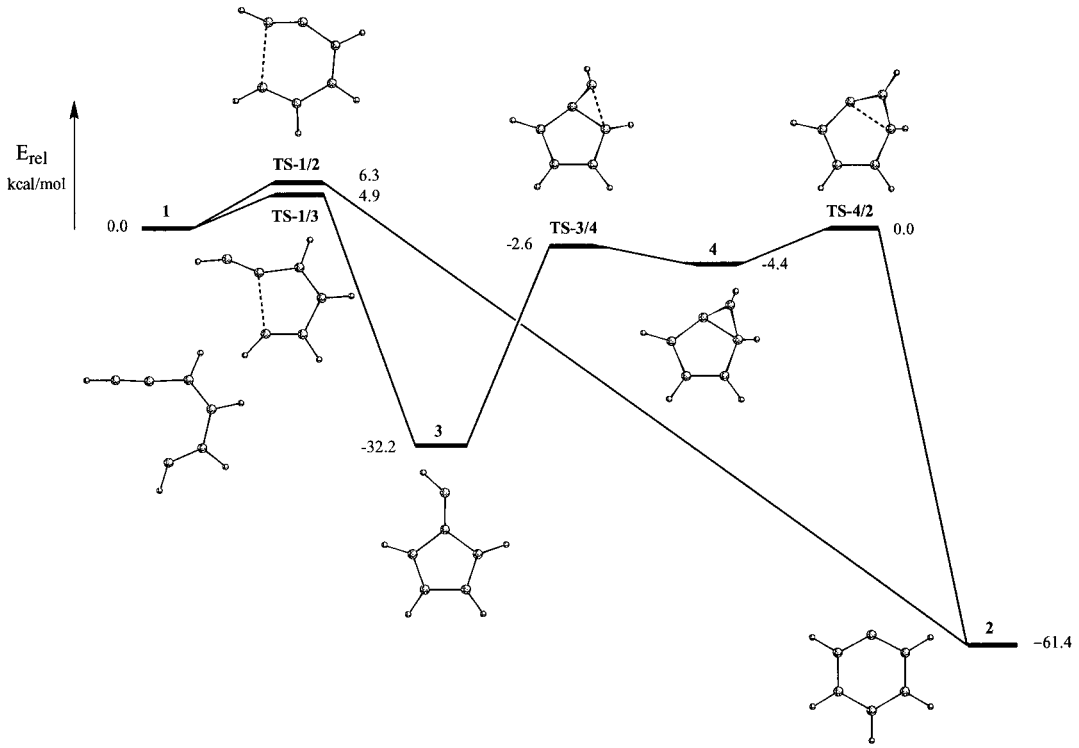

Figure 5. Schematic potential energy profiles showing the structures concerning the direct and stepwise pathways for the rearrangement of **1** to **2**. Relative energy values obtained from ZPVE-corrected approximated RCCSD(T)6-311+G(3df,2p) energies computed at the CASSCF/6-31G(d)-optimized geometries.

to enthalpy at 298 K leads to the $\Delta E^{\ddagger}$ and $\Delta H^{\ddagger}$ differences of 1.4 and 1.2 kcal/mol, respectively, between these two competing reactions. The $\Delta\Delta H^{\ddagger}$ (298 K) of 1.2 kcal/mol in favor of 5-*exo* cyclization of **1** is somewhat smaller than that obtained experimentally (1.7 kcal/mol)[21c] for *exo*- and *endo*-ring closures of radical **I**. To investigate if the activation entropy could reverse the preferred cyclization mode of **1** predicted on the grounds of the computed $\Delta U^{\ddagger}$, $\Delta E^{\ddagger}$, and $\Delta H^{\ddagger}$ (298 K), it is worthwhile to compare the Gibbs free energy of activation ($\Delta G^{\ddagger}$) obtained for each cyclization mode. At 298 K the $\Delta G^{\ddagger}$ for the 5-*exo* cyclization (5.8 kcal/mol) is found to be 1.5 kcal/mol lower than that for the 6-*endo* ring closure (7.3 kcal/mol). Thus, the activation entropy also favors 5-*exo* cyclization over the 6-*endo* ring closure. Even at high temperatures such as $T = 1450$ K the $\Delta G^{\ddagger}$ for 5-*exo* ring closure (14.0 kcal/mol) is predicted to be 3.4 kcal/mol lower than that for 6-*endo* cyclization (17.4 kcal/mol). Therefore, as in the case of the ring closure of the prototypical radical **I**, the predicted highly regioselective 5-*exo*-cyclization of **1** is due to favorable enthalpic and entropic factors associated with the formation of the smaller ring.

On the basis of the predicted preference for 5-*exo* cyclization of **1** to afford **3** over 6-*endo* ring closure to yield **2**, it seems unlikely that **2** is formed by simple 6-*endo* cyclization of **1**. Furthermore, this conclusion is confirmed by the results of RRKM computations based on the calculated $\Delta E^{\ddagger}$ and harmonic vibrational frequencies. The logarithm of *k(E)* versus *E* curves for the 5-*exo* and 6-*endo* cyclizations modes of **1**, computed by using eq 2, are shown in Figure 6. For the full range of internal energy excess with respect the ZPVE of **1** the RRKM-calculated rate constants reproduce the above predicted dominance of the 5-*exo* ring closure mode of **1**.

Finally, it is worth noticing that the DFT calculations based on the B3LYP method qualitatively agree with the RCCSD(T) calculations for the two cyclization modes of **1**. Thus, the activation parameters obtained from the B3LYP/6-311+G(3df,2p)//

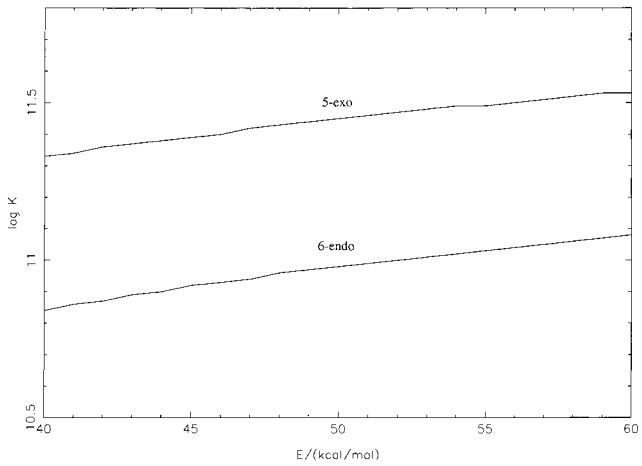

Figure 6. The logarithm of $k(E)$ versus E curves for the 5-*exo* and 6-*endo* cyclization of **1**, computed by using eq 2.

B3LYP/6-31G(d) energies in conjunction with the B3LYP/6-31G(d) harmonic vibrational frequencies (Table S3, Supporting Information) for the 6-*endo* ($\Delta E^{\ddagger} = 5.2$, $\Delta H^{\ddagger}$ (298 K) $= 4.5$, and $\Delta G^{\ddagger}$ (298 K) $= 6.0$ kcal/mol) and the 5-*exo* ($\Delta E^{\ddagger} = 4.5$, $\Delta H^{\ddagger}$ (298 K) $= 4.0$, and $\Delta G^{\ddagger}$ (298 K) $= 5.2$ kcal/mol) cyclization modes of **1** also favor the latter ring-closure mode.

B. Isomerization of 3 to 2. In light of the predicted preference for 5-*exo* cyclization of **1** to afford **3** over 6-*endo* ring closure to yield **2**, we investigated a possible stepwise mechanism for the **1** → **2** reaction involving the formation of radical **3** as a primary reaction product and the subsequent isomerization of **3** to **2**. The possibility of a hypothetical isomerization of **3** to **2** has not been considered in previous interpretations of experimental results. In principle, radical **3** might undergo an intramolecular radical addition to one of the two adjacent CC double bonds, leading to the highly strained bicyclo[3.1.0]hex-

3,5-dien-2-yl radical (**4**), which could undergo an opening of the three-membered ring to yield **2**.

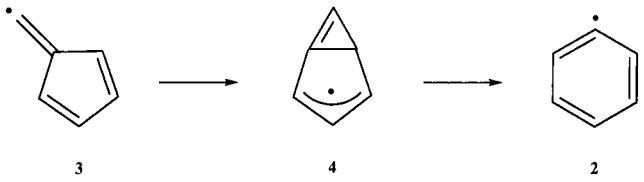

3 **4** **2**

A transition structure connecting **3** with **4**, labeled as **TS-3/4** in Figure 4, was located on the ground-state $C_6H_5^{\bullet}$ PES. The optimized geometries of **TS-3/4** and **4** are shown in Figure 4. In accordance with the expected high strain energy of the bicyclic intermediate **4**, as compared with **3**, at 0 K the **3** → **4** cyclization is predicted to be endoergic by 27.8 kcal/mol and to involve a $\Delta E^{\ddagger}$ of 29.6 kcal/mol. These results indicate that such an intramolecular radical addition is energetically unfavorable. However, according to all relative energies (ΔU, ΔE, ΔH, and ΔG) shown in Table 1, structures **TS-3/4** and **4** lie *below* the energy of **1**. Furthermore, at $T = 298$ and 1450 K the two-step reaction from **1** to **4** involves an overall $\Delta G^{\ddagger}$ (5.8 and 15.5 kcal/mol, respectively) that is lower than the ensuing $\Delta G^{\ddagger}$ (7.3 and 17.4 kcal/mol, respectively) for 6-*endo* ring closure of **1**. Thus, the two-step rearrangement **1** → **4** is favored over the 6-*endo* ring opening of **1**.

The ring opening of **4** leading to **2** was found to take place through the transition structure labeled as **TS-4/2** in Figure 4. At 0 K this ring opening is predicted to be exoergic by 57.0 kcal/mol and to involve a $\Delta E^{\ddagger}$ of only 4.4 kcal/mol. These results are in accordance with the expected high strain energy of **4**. It is worth noting that at $T = 298$ and 1450 K the ΔG of **TS-4/2** (1.6 and 16.8 kcal/mol, respectively) is predicted to be lower than that of **TS-1/2** (7.3 and 17.4 kcal/mol, respectively). Therefore, it can be concluded that the three-step pathway **1** → **3** → **4** → **2** is favored over the simple 6-*endo* cyclization **1** → **2**. Now we note that at ordinary temperatures (e.g., 298 K) the ΔG of **TS-1/3** is higher than that of **TS-4/2**, whereas at high temperatures (e.g., 1450 K) this relative ΔG ordering is reversed. These results indicate that, in passing from ordinary to high temperatures, the rate-determining step of the stepwise pathway **1** → **2** changes from being the 5-*exo* cyclization of **1** to be the three-membered ring opening of **4**.

Finally, it is worth mentioning that the DFT (B3LYP) calculations for the isomerization of **3** to **2** are in qualitative agreement with the results obtained with the RCCSD(T) method. Thus, the relative energies determined from the results of the B3LYP calculations (Table S3, Supporting Information) for **TS-3/4** (ΔE =-1.0, $\Delta H(298\ \text{K}) = -2.3$, and $\Delta G(298\ \text{K}) = 0.4$ kcal/mol), **4** ($\Delta E = -2.8$, $\Delta H(298\ \text{K}) = -3.8$, and $\Delta G(298\ \text{K}) = -1.5$ kcal/mol), and **TS-4/2** ($\Delta E = -0.1$, $\Delta H(298\ \text{K}) = -1.3$, and $\Delta G(298\ \text{K}) = 1.3$ kcal/mol), predict the stepwise pathway **1** → **3** → **4** → **2** to be preferred over the simple 6-*endo* cyclization **1** → **2**.

Summary and Conclusions

In the present study two distinct reaction pathways for the cyclization of the 1,3-hexadien-5-yn-1-yl radical, **1**, to yield phenyl radical, **2**, a key reaction in soot formation during fuel combustion processes, have been investigated computationally using ab initio quantum mechanical electronic structure methods. According to all barrier heights ($\Delta U^{\ddagger}$, $\Delta E^{\ddagger}$, $\Delta H^{\ddagger}$, and $\Delta G^{\ddagger}$) calculated from approximate RCCSD(T)/6-311+G(3df,2p) energies, obtained using essentially the G2M(RCC,MP2) scheme with optimized molecular geometries and harmonic vibrational frequencies determined at the CASSCF/6-31G(d) level, the 5-*exo* cyclization of **1** to (2,4-cyclopentadienyl)vinyl radical, **3**, is favored over the 6-*endo* cyclization to **2**. As in the case of the prototypical hex-5-enyl radical, **I**, the predicted highly regioselective 5-*exo* cyclization of **1** is due to favorable enthalpic and entropic factors associated with the formation of the smaller ring.

Contrary to common belief, the lowest-energy pathway for the reaction **1** → **2** is the 5-*exo* cyclization of **1** to **3** followed by cyclization of **3** to bicyclo[3.1.0]hex-3,5-dien-2-yl radical, **4**, and subsequent opening of the three-membered ring of **4** to yield **2**. The simple (one-step) 6-*endo* cyclization of **1** affording **2** requires a higher free energy of activation ($\Delta\Delta G^{\ddagger} = 1.5$ kcal/mol at 298 K) than such a stepwise mechanism. In passing from ordinary to high temperatures, the rate-determining step of the stepwise pathway **1** → **2** changes from being the 5-*exo* cyclization of **1** to be the opening of three-membered ring of **4**. These findings are in overall qualitative agreement with the results of DFT calculations based on B3LYP/6-311+G(3df,2p) energies in conjunction with optimized geometries and harmonic vibrational frequencies determined at the B3LYP/6-31G(d) level.

In light of the results of this investigation, the stepwise reaction pathway found between **1** and **2** should be included in the set of reactions used in detailed kinetic modeling of soot formation in shock-tube studies of acetylene pyrolysis.

Acknowledgment. This research was supported by the Spanish DGICYT (Grant PB98-1240-CO2-01. Additional support came from CIRIT (Grant 1999SGR00043). Calculations described in this work were performed on a HP9000 J282 workstation at the University of Barcelona and on the IBM SP2 at the Centre de Supercomputació de Catalunya (CESCA).

Supporting Information Available: Tables S1−S3 summarizing total energies, zero-point vibrational energies, absolute entropies, and thermal corrections to enthalpy calculated at different levels of theory of all structures reported in this paper (PDF). This material is available free of charge via the Internet at http://pubs.acs.org.

JA001011V